PERGAMON

Journal of Structural Geology 24 (2002) 1101–1107

JOURNAL OF STRUCTURAL GEOLOGY

www.elsevier.com/locate/jstrugeo

Microstructural and experimental constraints on the rheology of partially molten gabbro beneath oceanic spreading centers

Aaron S. Yoshinobu[a,*], Greg Hirth[b]

[a]*Department of Geosciences, Texas Tech University, Lubbock, TX 79409-1053, USA*
[b]*Department of Geology and Geophysics, Woods Hole Oceanographic Institute, Woods Hole, MA 02543, USA*

Received 7 February 2001; revised 30 April 2001; accepted 30 April 2001

Abstract

Flow laws for high-temperature creep of olivine, plagioclase, and diabase are used to place constraints on the rheology of partially molten lower oceanic crust. This analysis is motivated by the observation of olivine lattice preferred orientations and subgrain microstructures in oceanic gabbros that lack evidence for dislocation creep in coexisting plagioclase and pyroxene. Extrapolation of experimental flow laws indicates that at temperatures above 1100°C and stresses less than 10 MPa, olivine may be the weakest phase in rocks with gabbroic composition. By accounting for variations in the melt fraction (0–10%) and grain size of partially molten plagioclase aggregates we can constrain the rheological conditions where olivine deforms by dislocation creep while plagioclase deforms by diffusion creep. Calculated effective viscosities range from 10^{15} to 10^{19} Pa s; based on observations of the geometry of the partially molten zone beneath the East Pacific Rise and the microstructural and experimental constraints we favor a value of $\sim 10^{18}$ Pa s. This value approaches estimates for the viscosity of the upper mantle beneath ridge axes, but is significantly higher than previously suggested for the partially molten lower crust. Such high viscosities are inconsistent with ridge evolution models that require large amounts of lower crustal flow to accommodate melt redistribution. However, the results are compatible with recent models that favor local magma replenishment from the mantle at closely spaced intervals along the spreading center axis in a 2D, 'sheet-like' fashion.

Keywords: Rheology; Mid-ocean ridges; Ophiolites; Microstructures; Flow laws; Partially molten gabbro; Hypersolidus deformation

1. Introduction

The rheology of the partially molten lower oceanic crust, particularly beneath fast-spreading ridges, may control such ridge-scale phenomena as axial bathymetry (Wang et al., 1996) and lateral melt migration and redistribution during crustal accretion (Macdonald, 1998), yet direct observation and quantification of the parameters that control the rheology (i.e. stress, strain rate, melt fraction) of partially molten gabbros beneath oceanic spreading centers remains elusive. Seismic reflection/refraction and tomography studies of the East Pacific Rise (EPR) indicate that a thin melt lens is present directly beneath the base of Layer 2 (presumed sheeted dikes). The melt lens overlies a ~4-km-thick low-velocity zone (LVZ) interpreted to contain 0–50% melt (Detrick et al., 1987; Harding et al., 1989; Sinton and Detrick, 1992; Kent et al., 1994; Mainprice, 1997). Based on these observations, the LVZ has been suggested to be a zone of relatively low viscosity where large amounts of hypersolidus flow occurs to (a) accommodate along-strike crustal accretion away from the centers of ridge segments (Nicolas et al., 1996; Wang et al., 1996), and (b) advect crystallized magma down and away from the melt lens where crustal accretion occurs (Nicolas et al., 1993; Phipps-Morgan and Chen, 1993; Quick and Denlinger, 1993; Boudier et al., 1996; Macdonald, 1998).

One way of constraining the rheology of the partially molten lower crust is to extrapolate the results of rock deformation experiments to conditions appropriate for the lower oceanic crust. In this paper we summarize recent experimental rock deformation studies on gabbroic rocks and their constituent minerals and correlate the results of these experiments to microstructural observations from ophiolites and mid-ocean ridges to provide constraints on the rheology of the lower crust beneath a spreading ridge.

2. Conceptual model

Our analysis is motivated by the observation of olivine

* Corresponding author. Fax: +1-806-742-0100.
E-mail addresses: aaron.yoshinobu@ttu.edu (A.S. Yoshinobu), ghirth@whoi.edu (G. Hirth).

0191-8141/02/$ - see front matter
PII: S0191-8141(01)00094-3

subgrain microstructures indicative of dislocation creep in rocks that show no evidence for dislocation creep of coexisting plagioclase or pyroxene. Such textures, an example of which is shown in Fig. 1, have been described for samples from the Oman ophiolite (Benn and Allard, 1989; Boudier and Nicolas, 1995), the Southwest Indian Ridge (Dick et al., 1999), and the Tortuga ophiolite, southern Chile (Yoshinobu et al., 2000). These observations suggest that the stresses during the formation of the olivine microstructures were high enough to activate dislocation creep in olivine grains but not high enough to promote dislocation creep of the coexisting phases. These rocks have distinctive, well-developed magmatic foliations defined by aligned plagioclase laths, pyroxene crystals and elongate olivine crystals (Fig. 1a). Elongate pyroxene and plagioclase crystals often define a magmatic lineation. If the olivine microstructures were acquired during formation of the magmatic foliation (i.e. at hypersolidus conditions), then results from rock deformation experiments on high temperature creep of olivine crystals provide constraints on the rheologic parameters during formation of the magmatic foliation and lineation.

3. Application of experimental flow laws

We begin by assuming that the rheology of the partially molten gabbroic mush can be constrained by applying experimentally derived flow laws for gabbroic rocks and their constituent phases. In the end-member case that the material beneath the axis is completely solid, a flow law for high-temperature creep of dry diabase provides a constraint for the maximum effective viscosity (η_{eff} = stress/strain rate) at the ridge axis. We infer that the lower oceanic crust is primarily olivine gabbro, which is consistent with field observations from the Oman ophiolite, and direct sampling of the lower oceanic crust (e.g. Pallister and Hopson, 1981; Dick et al., 2000). We use diabase as a proxy for gabbro because virtually all deformation experiments are conducted on diabase, rather than coarse-grained gabbro, due to its optimal grain size/sample volume ratio for experiments. The flow law for dislocation creep of dry Columbia diabase is calculated using the power law relationship (Fig. 2a and b; Mackwell et al., 1998):

$$\dot{\epsilon} = A\sigma^n \exp(-Q/\mathrm{R}T) \quad (1)$$

where $\dot{\varepsilon}$ is strain rate, A an empirical constant, σ differential stress, n the stress exponent, Q activation energy, R the gas constant, and T temperature. We use the flow law for dry diabase because petrologic and geochemical evidence indicates that the lower crust is nominally dry prior to hydrothermal alteration and after extraction of MORB liquids (Hirth et al., 1998). The dry composition is particularly applicable to partially molten conditions where the majority of water present resides in the melt phase (Hirth and Kohlstedt, 1996). The flow law for dry diabase provides

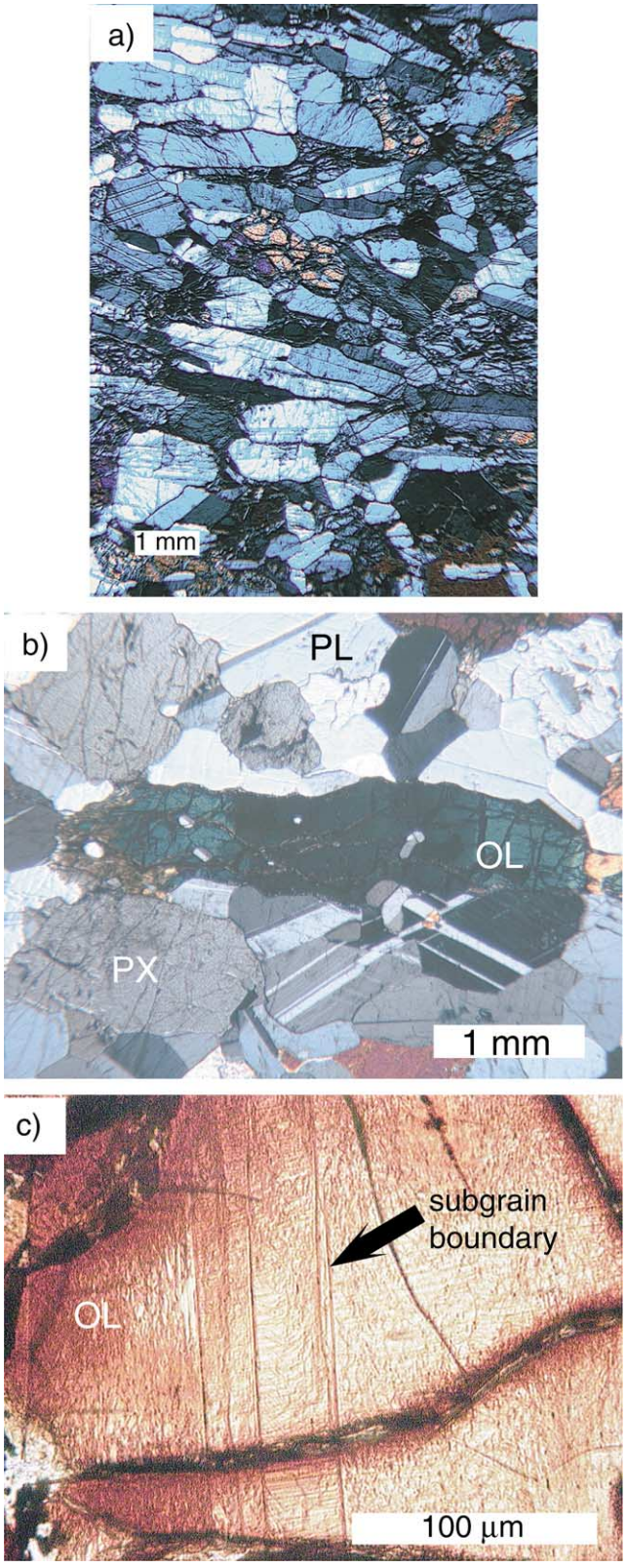

Fig. 1. (a) Photomicrograph of magmatic foliation from the lower crust of the Oman ophiolite. (b) Photomicrograph of olivine gabbro displaying olivine subgrain microstructures in cross-polarized light. (c) Photomicrograph of decorated thin section (see Jin et al., 1989) displaying dislocations and subgrain microstructures in olivine. OL = olivine, PL = plagioclase, PX = pyroxene.

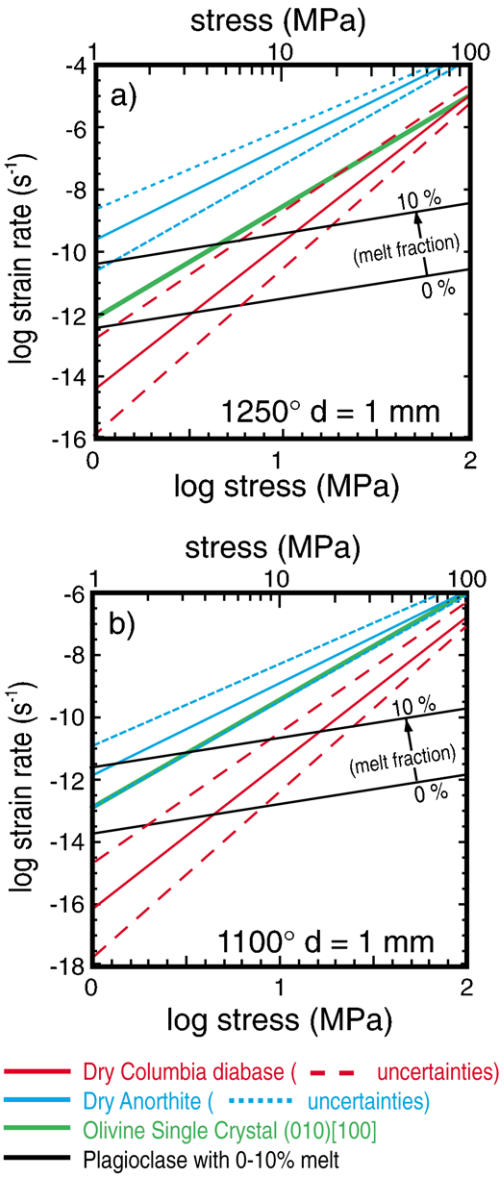

Fig. 2. Log stress–log strain-rate curves for olivine (green) deforming on the (010)[100] slip system (Bai et al., 1991), dry diabase (red; Mackwell et al., 1998), anorthite aggregates (blue; Rybacki and Dresen, 2000), and diffusion creep of plagioclase aggregates (black; Dimanov et al., 1998) with melt contents of 0–10% at (a) 1250°C and (b) 1100°C. Dashed lines represent uncertainties in the flow laws and reflect the uncertainties in the stress exponents of each dislocation creep flow law. Uncertainties in the olivine flow law are minimal and so are not plotted.

a constraint on the maximum strength of the lower crust beneath a ridge axis. If samples of the lower crust exhibit igneous textures and no evidence for dislocation creep, then the stress must have been lower than that necessary to activate dislocation creep in plagioclase, which is the framework phase in the Columbia diabase samples in Mackwell et al.'s experiments.

To evaluate dislocation creep in olivine single crystals, we use the composite flow law of Bai et al. (1991) for creep on (010)[100], the easiest slip system to activate at high temperatures (Raleigh, 1968; Durham and Goetze, 1977). The flow law has the form:

$$\dot{\epsilon} = A\sigma^n f_{O_2}^p \exp(-Q/RT) \quad (2)$$

where f_{O_2} is oxygen fugacity (set to QFM), and p is the oxygen fugacity exponent.

An additional constraint on the rheology of the partially molten lower crust is provided by experiments conducted on plagioclase aggregates with melt fractions (ϕ) ranging from 0.0 to 0.1 (Dimanov et al., 1998) in which deformation is accommodated by diffusion creep described by a flow law:

$$\dot{\epsilon} = A(\phi)\sigma^n d^m \exp(-Q/RT) \quad (3)$$

where ϕ is melt fraction, d grain size, and m the grain size exponent.

Strain rates predicted by extrapolating these flow laws to conditions appropriate for a ridge axis are shown for temperatures of 1100 and 1250°C in Fig. 2. The uncertainty inherent in this analysis is primarily due to the large extrapolation in stress (for the dislocation creep regime) or grain size (for the diffusion creep regime) from laboratory conditions to the earth. The uncertainties shown in Fig. 2 were obtained by recalculating the dislocation creep flow laws using the range in uncertainty for the stress exponent derived from the experiments. Because the experiments were conducted at similar temperatures to those beneath the ridge, our analysis is not significantly influenced by reported uncertainty in the activation energy (Q) in Eq. (1). At a temperature of 1250°C, the strain rate estimated for olivine deforming on its easiest slip system is greater than that predicted for dry diabase at stresses less than ~5 MPa (within the uncertainties of the Mackwell et al. flow law; Fig. 2a). At near-solidus temperatures (1100°C; Fig. 2b), olivine deforms faster than dry diabase for stresses less than ~25 MPa. Strain rates calculated using the flow laws for diffusion creep of dry plagioclase aggregates with porosities of 0.01 to 0.10 and 1 mm crystal size are also shown in Fig. 2. A grain size of 1 mm was chosen based on microstructural observations of Oman gabbros (e.g. Nicolas and Ildefonse, 1996). At the lower end of the stress range shown in Fig. 2a and b (~1–10 MPa), the strain rate predicted for diffusion creep of plagioclase is similar to that estimated for olivine deforming on its easiest slip system.

At face value, the relationships shown in Fig. 2 are consistent with microstructural observations that suggest that under some conditions it is possible for a plagioclase matrix to deform by diffusion creep while olivine grains deform by dislocation creep. By contrast, strain rates predicted by extrapolation of a recently determined dislocation creep flow law for fine-grained anorthite aggregates (Rybacki and Dresen, 2000) range from 10^{-9} to 10^{-6} s^{-1}, considerably greater than those predicted for dislocation creep of dry diabase and olivine single crystals, or diffusion creep of plagioclase aggregates with variable melt fractions (Fig. 2). The large discrepancy in strain rate predicted by the fine-grained anorthite flow law and the diabase flow law is a

manifestation of the difference in the stress exponent reported for these studies. Rybacki and Dresen determined $n = 3 \pm 0.4$, while Mackwell et al. measured $n = 4.7 \pm 0.6$. Thus, while the strength of these materials in the lab is similar, the calculated strain rates diverge when the flow laws are extrapolated to significantly lower stresses. It is possible that the lower value of n determined by Rybacki and Dresen reflects a component of diffusion creep and/or grain boundary sliding (e.g. Hirth and Kohlstedt, 1995; Goldsby and Kohlstedt, 1997). Their experiments were conducted near the transition between the two dominant creep mechanisms.

4. Discussion

4.1. Timing of dislocation creep in olivine

Olivine single crystal flow laws can be used to constrain the rheology of partially molten gabbro if the olivine microstructures were acquired during formation of the magmatic foliation. Several microstructural observations indicate that olivine deforms by dislocation creep at hypersolidus conditions. First, samples that display a strong plagioclase shape and lattice preferred orientation (SPO and LPO), such as in Fig. 1a, commonly also have an olivine LPO suggesting that the olivine microstructure formed at the same time as the lineation and foliation in the olivine gabbro. Studies of the LPO's of olivines from the lower crust of the Oman ophiolite show a strong maximum of *a*-axes parallel to lineations defined by plagioclase laths (Boudier and Nicolas, 1995). Therefore, because microstructural criteria such as preferred mineral orientation defined by laths of undeformed plagioclase, straight crystal boundaries, and primary zoning (Nicolas and Ildefonse, 1996; Paterson et al., 1998; Vernon, 2000) are consistent with the formation of the gabbro foliation and lineation at hypersolidus conditions, then it is probable that the olivine microstructures are hypersolidus in origin as well. Our microstructural observations of olivine microstructures and plagioclase SPO's on samples from the Southwest Indian Ridge (Dick et al., 1999) are also consistent with their formation at hypersolidus conditions. One caveat to this interpretation is that the olivine grains could be xenocrysts of deformed mantle peridotite incorporated into the ascending magmas (Boudier and Nicolas, 1995). However, if this were the case, it is surprising that the olivine xenocrysts maintain a LPO and SPO (e.g. Boudier and Nicolas, 1995).

Although subgrains may form at relatively low strains, the presence of a well-defined LPO suggests that strains must have been at least ~20% (e.g. Zhang and Karato, 1995). At these strains, if the subgrain microstructure developed at subsolidus conditions, we would expect to observe dislocation creep microstructures in plagioclase. Thus, we conclude that the subgrain microstructures in olivine were acquired when the magmatic foliation formed during hypersolidus strain of the crystal mush, containing 1–10% melt (e.g. Fig. 2; Dimanov et al., 1998).

4.2. Estimates of strain rate and effective viscosity

Evidence for dislocation creep of olivine at hypersolidus conditions provides a constraint for estimating strain rates and effective viscosities of partially molten gabbro. We interpret that the olivine grains deform plastically as a result of applied tractions imposed by the adjacent plagioclase and pyroxene crystals during flow of the crystal mush. By assuming that the rheology of the olivine grains can be determined by the flow law for olivine on its easiest slip system ((010)[100]), estimates for effective viscosity (η_{eff} = stress/strain rate) can be calculated. Assuming stresses in the range of 1–10 MPa, calculated strain rates are 10^{-12} to 10^{-9} s^{-1}; corresponding to effective viscosities of 10^{15} to 10^{19} Pa s. The influence of temperature on the effective viscosities of olivine single crystals is shown as a function strain rate in Fig. 3 using the flow law of Bai et al. (1991). At face value, the point at which the olivine flow law intersects the diabase flow law (Fig. 2) represents the stress below which only olivine will deform by dislocation creep. However, approaching this stress, the plagioclase should also display evidence for dislocation creep. Based on the lack of any prominent dislocation creep in the plagioclase, we favor a stress estimate of ~1 MPa, resulting in strain rates of 10^{-12} to 10^{-13} s^{-1} at 1250 and 1100°C, respectively. As shown in Fig. 3, this range of conditions corresponds to effective viscosities of 10^{18} to 10^{19} Pa s.

Knowledge of the geometry of the partially molten zone can provide further constraints on the range of strain rates affecting the lower crust. Recent tomography studies of the oceanic crust near 9°30′N along the EPR indicate that melt

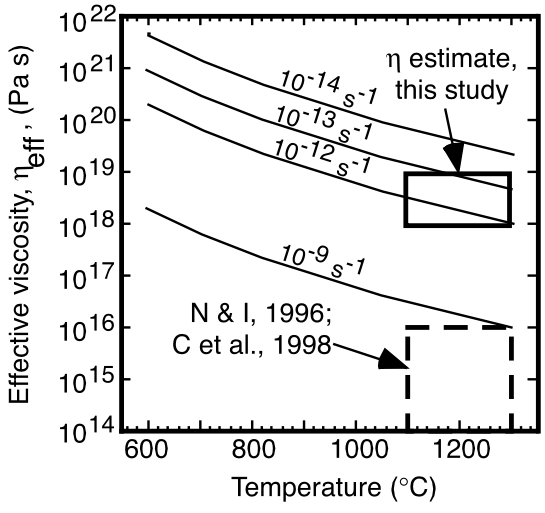

Fig. 3. Effective viscosity versus temperature for olivine single crystals deforming on the (010)[100] slip system at different strain rates. The viscosity window estimated in this study is outlined with the solid box. The viscosity window calculated by Nicolas and Ildefonse (1996) and used in the numerical modeling study of Chenevez et al. (1998) is also shown.

is present in a 'bell-jar' shaped region that is 5–7 km wide just below the melt lens at the base of the sheeted dikes and ~20 km wide at the Moho transition zone (Dunn et al., 2000). The melt fraction within this region could range from 1 to 38%, depending on melt/crystal topology and possible anelastic effects (Dunn et al., 2000). Assuming that extension is distributed homogeneously over the entire 4-km-thick lower crust, the strain rate in this region can be estimated using the relationship strain rate = spreading rate/width of deforming lower crust (e.g. Ramsay and Huber, 1983). For the EPR this gives strains rates in the order of $10^{-12}\ s^{-1}$, which is consistent with our estimates based on the combination of microstructural analyses and experimental flow laws.

Our strain rate estimates for partially molten gabbro are lower than those favored by Nicolas and Ildefonse (1996). Based on microstructural observations of samples collected from the Oman ophiolite, Nicolas and Ildefonse (1996) estimated strain rates and viscosity of the partially molten lower crust using a diffusion-limited grain-boundary sliding flow law. For effective grain boundary diffusion distances of 0.1 and 1.0 mm, they calculated strain rates of $\sim 10^{-9}$ and $10^{-12}\ s^{-1}$, respectively. Using a strain rate of $10^{9}\ s^{-1}$ and assuming differential stresses in the range of $1 < \sigma < 10$ MPa, they calculated η_{eff} of 10^{14}–10^{16} Pa s, which is broadly consistent with our calculations for a minimum viscosity. Strain rates of $10^{-12}\ s^{-1}$ yield η_{eff} values of 10^{18}–10^{19} Pa s, but were argued to be too low by Nicolas and Ildefonse (1996) because these values approach upper mantle effective viscosities.

Nicolas and Ildefonse (1996) favor lower crustal viscosities of 10^{14}–10^{15} Pa s motivated by models for the accretion of the lower ocean crust in which deformation is driven by active mantle upwelling (i.e. Nicolas et al., 1993). However, strain rates on the order of $10^{-9}\ s^{-1}$ are unlikely, even for this end-member crustal accretion scenario. Again assuming that deformation is accommodated throughout the 4 km thickness of the partially molten lower crust, to achieve strain rates of $\sim 10^{-9}\ s^{-1}$ the mantle upwelling rates, and therefore divergent mantle flow rates, must be $\sim 130\ m\ year^{-1}$. Such velocities are several orders of magnitude greater than even the most extreme calculations of buoyancy-driven mantle upwelling rates (e.g. Buck and Su, 1989). Geologically motivated models for crustal flow driven by active mantle upwelling have been presented by Chenevez et al. (1998). Models with crustal viscosities of $\sim 10^{15}$ Pa s exhibit flow lines similar to those inferred for magmatic-suspension flow in the Oman ophiolite. However, the maximum active mantle flow velocities used in these models are $0.5\ m\ year^{-1}$, resulting in shear strain rates on the order of $(0.5\ m\ year^{-1})/(4000\ m) = 4 \times 10^{-12}\ s^{-1}$. Thus, the inferred stress level for these numerical experiments is in the range of $(10^{15}\ Pa\ s) \times (4 \times 10^{-12}\ s^{-1}) = 4000$ Pa, which is several orders of magnitude too low to promote dislocation creep in olivine single crystals or appreciable rates of diffusion creep in rocks with ~10% melt (Fig. 2).

Given the microstructural and experimental constraints discussed here, we suggest that crustal accretion at fast spreading rate/high magma supply ridges occurs along axis throughout the lower crust. Based on the seismic tomography noted above and ophiolite studies it is apparent that magma emplacement occurs in at least two regions beneath the ridge axis: in a shallow crustal melt lens (Detrick et al., 1987; Kent et al., 1994) and in the Moho transition zone (Boudier et al., 1996; Kelemen et al., 1997; Dunn et al., 2000). Based on the preservation of fine-scale modal layering in the lower gabbros of the Oman ophiolite and geochemical evidence, Korenaga and Kelemen (1997; see also Kelemen and Aharonov, 1998) have proposed that magma accretion may occur throughout the lower crust. In this scenario, large shear strains and fast deformation velocities are not required to translate crystallized material down and away from the melt lens, redistributing magma along the axis in the lower crust. Therefore, because the olivine microstructures and experimental constraints indicate that strain rates are relatively slow and effective viscosities relatively high, flow in the lower crust is probably not an effective means of redistributing magma along the ridge axis from spaced magmatic centers (e.g. Wang et al., 1996; Macdonald, 1998). These conclusions are more consistent with the notion that magma accretion occurs along the entire ridge axis in a 2D, sheet-like fashion.

5. Conclusions

Based on the analysis of experimental rock deformation results and microstructural observations from ophiolites and the South West Indian Ridge, we draw the following conclusions:

1. Some oceanic gabbros exhibit dislocation creep microstructures in olivine crystals while coexisting plagioclase and pyroxene show no evidence for dislocation creep. These microstructures are interpreted to form at hypersolidus conditions.
2. At temperatures above 1100°C and stresses less than 10 MPa, dislocation creep strain rates for olivine single crystals range from 10^{-9} to $10^{-12}\ s^{-1}$, up to two orders of magnitude higher than for dry diabase, indicating that olivine is the weakest phase at these conditions. Strain rates predicted for diffusion creep of partially molten plagioclase aggregates at these conditions are similar to those predicted for dislocation creep of olivine single crystals. These experimental results are consistent with microstructural observations from oceanic gabbros.
3. Effective viscosities at these stresses and strain rates range from 10^{15} to 10^{19} Pa s. Based on seismic constraints for the geometry of the partially molten lower crust at the East Pacific Rise and the known spreading rates, we suggest that strain rates in the partially

molten lower crust are $\sim 10^{-12}\ s^{-1}$ and viscosities are on the order of 10^{18} Pa s.

An effective viscosity in the order of 10^{18} Pa s may limit downward and/or along-axis crustal flow, making it difficult for large-scale redistribution of magma to occur by hypersolidus flow within the axial crust. A relatively high crustal viscosity may therefore favor magma chamber replenishment at closely spaced intervals along the ridge axis rather than through single magmatic centers (i.e. 3D upwelling) and large-scale redistribution of magma along axis.

Acknowledgements

We thank Ron Vernon for his career-long contribution to the understanding of microstructures and their application to unraveling tectonic problems. Scott Johnson and Mike Williams put together a fantastic symposium on microstructural processes in Ron's honor at the 15th Australian Geological Convention and we appreciate and acknowledge the opportunity to take part in this wonderful meeting. Yoshinobu thanks the second author for introducing him to the application of experimental rock deformation studies to naturally deformed rocks. Brad Hacker and Tracy Rushmer are thanked for their encouraging and constructive reviews. We thank Peter Kelemen, Greg Harper, Scott Paterson, Keegan Schmidt, and fellow ODP Leg 176ers Henry Dick, Benoit Ildefonse, Bobbie John, and Pat Trimby for insightful discussions regarding the nature of deformation in the oceanic lower crust. Our microstructural and field studies of oceanic gabbros have been supported by the JOI-USSSP, the National Geographic Society, and NSF Grants OCE-9730018 (Yoshinobu) and OCE-9819666 and OCE-9626930 (Hirth).

References

Bai, Q., Mackwell, S.J., Kohlstedt, D.L., 1991. High-temperature creep of olivine single crystals, 1. Mechanical results for buffered samples. Journal of Geophysical Research 96, 2441–2463.

Benn, K., Allard, B., 1989. Preferred mineral orientations related to magmatic flow in ophiolite layered gabbros. Journal of Petrology 30, 925–946.

Boudier, F., Nicolas, A., 1995. Nature of the Moho transition zone in the Oman ophiolite. Journal of Petrology 36, 777–796.

Boudier, F., Nicolas, A., Ildefonse, B., 1996. Magma chambers in the Oman ophiolite: fed from the top or from the bottom? Earth and Planetary Science Letters 144, 239–250.

Buck, W.R., Su, W., 1989. Focused mantle upwelling below mid-ocean ridges due to feedback between viscosity and melting. Geophysical Research Letters 16, 641–644.

Chenevez, J., Machetel, P., Nicolas, A., 1998. Numerical models of magma chambers in the Oman ophiolite. Journal of Geophysical Research 103, 15443–15456.

Detrick, R.S., Buhl, P., Vera, E., Mutter, J., Orcutt, J., Madsen, J., Brocher, T., 1987. Multi-channel seismic imaging of a crustal magma chamber along the East Pacific Rise. Nature 326, 35–42.

Dick, H.J.B., Leg 176 Scientific Party, 2000. A long in situ section of the lower ocean crust: results of ODP Leg 176 drilling at the Southwest Indian Ridge. Earth and Planetary Science Letters 179, 31–51.

Dick, H.J.B., Natland, J.H., Miller, D.J., et al., 1999. Proc. ODP, Init. Repts., 176 [CD-ROM]. Available from: Ocean Drilling Program, Texas A&M University, College Station, TX 77845-9547, USA.

Dimanov, A., Dresen, G., Wirth, R., 1998. High-temperature creep of partially molten plagioclase aggregates. Journal of Geophysical Research 103, 9651–9664.

Dunn, R.A., Toomey, D.R., Solomon, S.C., 2000. Three-dimensional seismic structure and physical properties of the crust and shallow mantle beneath the East Pacific Rise. Journal of Geophysical Research 105, 23537–23556.

Durham, W.B., Goetze, C., 1977. Plastic flow of oriented single crystals of olivine, 1. Mechanical data. J. Geophysical Research 82, 5737–5753.

Goldsby, D., Kohlstedt, D.L., 1997. Grain boundary sliding in fine-grained ice I. Scr. Mater. 37, 1399–1406.

Harding, A.J., Orcutt, J.A., Kappus, M.E., Vera, E.E., Mutter, J.C., Buhl, P., Detrick, R.S., Brocher, T.M., 1989. Structure of young oceanic crust at 13°N on the East Pacific Rise from expanding spread profiles. Journal of Geophysical Research 94, 12163–12196.

Hirth, G., Kohlstedt, D.L., 1995. Experimental constraints on the dynamics of the partially molten upper mantle: deformation in the diffusion creep regime. Journal of Geophysical Research 100, 1981–2001.

Hirth, G., Kohlstedt, D.L., 1996. Water in the oceanic upper mantle: implications for rheology, melt extraction and the evolution of the lithosphere. Earth and Planetary Science Letters 144, 93–108.

Hirth, G., Escartin, J., Lin, J., 1998. The rheology of the lower oceanic crust: implications for lithospheric deformation at mid-ocean ridges. In: Buck, W.R., Delaney, P.T., Karson, J.A., Lagabrielle, Y. (Eds.). Faulting and Magmatism at Mid-Ocean Ridges. AGU Monograph 106, pp. 291–304.

Jin, Z.-M., Green, H.W., Borch, R.S., 1989. Microstructures of olivine and stresses in the upper mantle beneath Eastern China. Tectonophysics 169, 23–50.

Kelemen, P.B., Aharonov, E., 1998. Periodic formation of magma fractures and generation of layered gabbros in the lower crust beneath oceanic spreading ridges. In: Buck, W.R., Delaney, P.T., Karson, J.A., Lagabrielle, Y. (Eds.). Faulting and Magmatism at Mid-Ocean Ridges. AGU Monograph 106, pp. 267–289.

Kelemen, P.B., Koga, K., Shimizu, N., 1997. Geochemistry of gabbro sills in the crust-mantle transition zone of the Oman Ophiolite: implications for the origin of the oceanic lower crust. Earth and Planetary Science Letters 146, 475–488.

Kent, G.M., Harding, A.J., Orcutt, J.A., Detrick, R.S., Mutter, J.C., Buhl, P., 1994. Uniform accretion of oceanic crust south of the Garret transform at 14°15′S on the East Pacific Rise. Journal of Geophysical Research 99, 9097–9116.

Korenaga, J., Kelemen, P.B., 1997. Origin of gabbro sills in the Moho transition zone of the Oman ophiolite: implications for magma transport in the oceanic lower crust. Journal of Geophysical Research 102, 27729–27749.

Macdonald, K.C., 1998. Linkages between faulting, volcanism, hydrothermal activity and segmentation on fast spreading centers. In: Buck, W.R., Delaney, P.T., Karson, J.A., Lagabrielle, Y. (Eds.). Faulting and Magmatism at Mid-Ocean Ridges. pp. 27–58 AGU Monograph 106.

Mackwell, S.J., Zimmerman, M.E., Kohlstedt, D.L., 1998. High-temperature deformation of dry diabase with application to tectonics on Venus. Journal of Geophysical Research 103, 975–984.

Mainprice, D., 1997. Modeling the anisotropic seismic properties of partially molten rocks found at mid-ocean ridges. Tectonophysics 2791, 161–179.

Nicolas, A., Ildefonse, B., 1996. Flow mechanisms and viscosity in basaltic magma chambers. Geophysical Research Letters 23, 2013–2016.

Nicolas, A., Freydier, C., Godard, M., Vauchez, A., 1993. Magma chambers at oceanic ridges: how large? Geology 21, 53–56.

Nicolas, A., Boudier, F., Ildefonse, B., 1996. Variable crustal thickness in

the Oman ophiolite: Implications for oceanic crust. Journal of Geophysical Research 101, 17941–17950.

Pallister, J.S., Hopson, C.A., 1981. Samail ophiolite plutonic suite: field relations, phase variation, cryptic variation and layering, and a model of a spreading ridge magma chamber. Journal of Geophysical Research 86, 2593–2644.

Paterson, S.R., Fowler, T.K., Schmidt, K.L., Yoshinobu, A.S., Yuan, E.S., Miller, R.B., 1998. Interpreting magmatic fabrics in plutons. Lithos 44, 53–82.

Phipps-Morgan, J., Chen, Y.J., 1993. The genesis of oceanic crust: magma injection, hydrothermal circulation, and crustal flow. Journal of Geophysical Research 98, 6283–6298.

Quick, J.E., Denlinger, R.P., 1993. Ductile deformation and the origin of layered gabbro in ophiolites. Journal of Geophysical Research 98, 14015–14027.

Raleigh, C.B., 1968. Mechanisms of plastic deformation of olivine. Journal of Geophysical Research 73, 5391–5406.

Ramsay, J.G., Huber, M.I., 1983. The Techniques of Modern Structural Geology. Volume 1: Strain Analysis. Academic Press, San Diego, CA.

Rybacki, E., Dresen, G., 2000. Dislocation and diffusion creep of synthetic anorthite aggregates. Journal of Geophysical Research 105, 26017–26036.

Sinton, J.M., Detrick, R.S., 1992. Mid-ocean ridge magma chambers. Journal of Geophysical Research 97, 197–216.

Vernon, R.H., 2000. Review of microstructural evidence of magmatic and solid-state flow. Electronic Geosciences, 5/2.

Wang, X.C., Cochran, J.R., Barth, G.A., 1996. Gravity anomalies, crustal thickness and the pattern of mantle flow at the fast spreading East Pacific Rise, 9–10°N: evidence for three-dimensional upwelling. Journal of Geophysical Research 101, 17927–17940.

Yoshinobu, A.S., Pignotta, G., Schmidt, K.L., 2000. Geometry of intrusion and magma migration in the Tortuga ophiolite, Chilean Tierra del Fuego. Geological Society of America Abstracts With Programs 32, 236.

Zhang, S., Karato, S., 1995. Lattice preferred orientation of olivine aggregates deformed in simple shear. Nature 37, 774–777.